



HAL
open science

High-Bandwidth 3-D Multitrap Actuation Technique for 6-DoF Real-Time Control of Optical Robots

Edison Gerena, Stéphane Régnier, Sinan Haliyo

► **To cite this version:**

Edison Gerena, Stéphane Régnier, Sinan Haliyo. High-Bandwidth 3-D Multitrap Actuation Technique for 6-DoF Real-Time Control of Optical Robots. *IEEE Robotics and Automation Letters*, 2019, 4 (2), pp.647-654. 10.1109/lra.2019.2892393 . hal-02016632

HAL Id: hal-02016632

<https://hal.sorbonne-universite.fr/hal-02016632v1>

Submitted on 12 Feb 2019

HAL is a multi-disciplinary open access archive for the deposit and dissemination of scientific research documents, whether they are published or not. The documents may come from teaching and research institutions in France or abroad, or from public or private research centers.

L'archive ouverte pluridisciplinaire **HAL**, est destinée au dépôt et à la diffusion de documents scientifiques de niveau recherche, publiés ou non, émanant des établissements d'enseignement et de recherche français ou étrangers, des laboratoires publics ou privés.

High-bandwidth 3D Multi-Trap Actuation Technique for 6-DoF Real-Time Control of Optical Robots

Edison Gerena , Stéphane Régnier and Sinan Haliyo

Abstract—Optical robots are micro-scale structures actuated using laser trapping techniques. However, the lack of robust and real-time 3D actuation techniques reduces most applications to planar space. We present here a new approach to generate and control several optical traps synchronously in 3D with low latency and high bandwidth (up to 200 Hz). This time-shared technique uses only mirrors, hence is aberration-free. Simultaneous traps are used to actuate optical robots and provide 6-DoF telemanipulation. Experiments demonstrate the flexibility and dexterity of the implemented user control, paving the way to novel applications in micro-robotics and biology.

Index Terms—Micro/Nano Robots, Biological Cell Manipulation, Telerobotics and Teleoperation

I. INTRODUCTION

MOBILE micro-robots promising access to intangible scales brings revolutionary potential to a vast amount of biological applications, ranging from minimally invasive unicellular surgery to exploration of fundamental biological phenomena [1]. Optical trapping is a practical mean for actuating these tiny micro-machines in confined environments, such as lab-on-chip devices. They use the optical force generated by the energy and momentum exchange between light and particles to drive the mechanical motions of micro objects with nanometer resolution [2]. Using diffractive optical elements or active components, multiple traps can be generated from a single source, allowing simultaneous manipulation of several independent samples or applying torques on non-spherical objects.

Optical manipulation has become a popular tool for manipulating single biological samples, successfully demonstrated in a large range of in-vivo [3] and in-vitro [4] experiments such as the trapping of red blood cells in living animals [5], the immobilization of bacterial cells for nanoscopy [6] and cell rotation for tomographic imaging [7], among others. Usually, these optical traps are used directly to manipulate the object of interest. This approach suffers mainly from two issues:

the exposure of biological samples to the laser beams can be damaging, and the quality of the trap strongly depends on the shape, material and the refraction index of the target, hence it's difficult to reliably hold organic samples.

For these reasons, indirect manipulation methods have been proposed, where optically trapped structures are used as tools. Additionally, implementing sensing, actuation and feedback control leverage these structures as *optical robots*. The most basic and common example of such a tool is a polystyrene bead attached to the target sample [3]. Multiple beads arranged into gripper formations for the manipulation of cells are then explored [8]. Recent advances in microscale additive fabrication processes [9] have led the way to novel examples of micro-mechanisms actuated through optical trapping. These more complex structures are designed with attached spherical parts serving as optically trappable handles. Eventually, using an appropriate mix of surfactants or nano-materials, some interesting functions are demonstrated: a micro-pump [10]; a pH measurement gel-microtool by connecting micro-beads impregnated with indicators [11]; a micro-tool integrating a silicon nano-wire for temperature sensing [12]; a surface scanning probe [13]; a micro-robot with syringe function [14]; an optical screw-wrench for micro-assembly [15].

The use of intermediate tools clearly widens the scope of optical trapping. Controlling these so-called optical robots requires the synchronous control of each handle. This in turn requires a precise control of the laser exposure and the trajectory of individual traps. Also, the overall stability depends on guaranteeing the same amount of power is transmitted at each trap, regardless of its position. This is only possible on an efficient, high-bandwidth and low-latency system [16].

These constraints are quite difficult to satisfy, therefore most optical robots are confined in 2D space in the optical plane (two translations and a rotation), limiting the applications where 3D controlled motion is crucial, such as cell orientation for micro-injection, polar-body biopsy, nuclear transplantation or 3D tomographic imaging [17].

The main aim of this paper is to present a new design of optical actuation to generate and control several simultaneous traps in 3D space. This design is solely based on mirrors, thus maximizing the optical efficiency. The choice of components with very high response times lowers latency and increases considerably the bandwidth for the control. Following a literature survey on multi-trap solutions, the proposed system

This work was

supported by the French National Research Agency through the ANR-IOTA project (ANR-16-CE33-0002-01), and partially by the French government research program "Investissements d'avenir" through the Robotex Equipment of Excellence (ANR-10-EQPX-44).

¹All authors are with Sorbonne Université, CNRS, Institut des Systèmes Intelligents et de Robotique UMR 722, 4 place Jussieu, 75005 Paris, France. {gerena, regnier, haliyo}@isir.upmc.fr

DigitalObjectIdentifier(DOI):10.1109/LRA.2019.2892393

is described here. Then, its capabilities are demonstrated by controlling simultaneously thirteen individual objects in 3D. Finally, its real-time capabilities are depicted in a teleoperated scenario, controlling true 6D motions of optical robots.

II. BACKGROUND AND RELATED WORK

Controlling the 3D motion of non-spherical objects (like cells, or synthetic robots) where optical handles are rigidly linked is much more demanding than controlling separate and individual beads. Relative deviations in the position of each trap will affect the stability of the whole structure and the force on each trap will interfere with the dynamics of the motion, as well as differences in the power distribution between traps. The generation of several simultaneously trapping points using a single laser source can be achieved using spatial or temporal sharing methods with their specific strengths and limitations. Table I summarizes the properties of some significant methods.

In spatial-sharing, using the light-diffraction, the beam is split on several less powerful beams. This requires a diffractive optical component such as a *Spatial Light Modulator (SLM)*. Holographic optical tweezers (*HOT*) [18] or Generalized Phase Contrast (*GPC*) [19] are one of the most common techniques for creating multiple traps in 3D. However, calculating the hologram for a given number of traps in space is quite processor intensive. Liquid crystal components have also a relatively low response time. Hence, it's currently quite impossible to obtain sufficient bandwidth for real-time operation using spatial sharing. Recently, some studies utilizing HOT systems for rotational motions are reported. 2D actuation of an optical micro-robot is presented [20]. Limited by the response time of the *SLM* (80 ms) and the stability of the traps, the maximum control frequency of the microrobot is 3 Hz. 3D rotation control of single live mammalian cells was reported [21]. Nonetheless, out-of-plane rotation speed of the cell and the traps are different with an important delay time of 1 to 5 seconds. Multiple degrees of freedom in HOT systems are also possible through wave-front shaping, using vortex [22], Laguerre-Gaussian [23], and other beam shapes [24], [25]. Although these SLM-based techniques represent elegant solutions for the 3D motion or rotations, the extensive computational cost and complexity of trajectory control make their implementation in real-time scenarios a very difficult task.

On the other hand, multiple stable trapping points can be created by rapidly deflecting a laser beam among a set of positions. In these temporal-sharing methods the frequency

of the trap scanning should be faster than the Brownian relaxation time of the trapped objects [26]. Usually these methods use a scanning mirror system [27] or an acousto-optic deflector (*AOD*) [28]. Time-shared methods are suitable for controlled manipulation under real-time automatic/interactive control. Nevertheless, these are commonly limited to two dimensions.

Using a motorized objective or a z stage, the axial position of the beam can be controlled [29], [30], [31]. However, the inertia of such a system makes the synchronization of axial and planar motions a very difficult task. Some interesting approaches are reported to overcome this limitation. By combining a deformable mirror and acousto-optic deflector, a 3D steering system for single particle manipulation is presented, but no multi-trap capability has been reported [32]. An oscillating optical trap is used to rotate rod-shaped bacterial cells with respect to the optical axis [33]. The oscillating trap was produced by means of a galvanometric mirror and the angle of rotation is determined by the amplitude of the oscillation. An electrically focus-tunable lens combined with a two-axis steering mirror is proposed [34], [35], but its delayed response and distortion make it impossible to control 3D rotations accurately. A combination of a mirror galvanometer with a *GPC* to manipulate a micro-tool was proposed [36]. The *GPC* generates fixed laser traps and the galvanometer is used to manipulate the overall configuration. The trapping force induced by *GPC* is weaker than what can be obtained directly by a mirror, hence the motion is quite limited and confined in the optical plane. As a workaround for the axial motion, an articulated robot with an out-of-plane mobility of an appendix using AOD is proposed [37]. The precise and stable control of this DoF is a complex endeavour as it is controlled through handles on the structure in the same focal plane.

The lack of high bandwidth and low latency systems makes precise real-time control a challenging task, limiting the potential of optical robots that interact in a micro-world with high dynamics effects. An alternative design introducing a time-shared scanning technique for 3D multi-trap actuation is presented next. This system is based on the synchronization of a deformable mirror and a steering mirror and allows simultaneous control of focal and planar positions. This approach combines the efficiency of optical components with high reflectance and low latency response times.

III. HIGH-BANDWIDTH 3D MULTI-TRAP ACTUATION

The efficiency of an optical trap is related to the intensity distribution near the focal point. This diffraction-limited spot size is usually obtained by using an objective lens of high numerical aperture (*NA*). The location of the trap is determined by the angle of incidence and the degree of collimation of the laser beam and its stability is very dependent on the quality of the beam that reaches the entrance of the microscope objective. However, given the correlation between the beam that reaches the objective and the focal point, it is difficult to change the 3D position of the trap without distorting its shape and introducing aberrations that will degrade its performance [38].

To overcome these constraints in all three dimensions, a mirror galvanometer is used for the in-plane ($x - y$) scanning.

TABLE I
COMPARISON OF 3D MULTI-TRAP ACTUATION METHODS

Method	Response time	Bandwidth	Trajectory computation	Trap force
GPC	High	Low	Medium*	Weak
HOT	High	Low	Complex*	Weak
MO + SM	Very High	High	Simple	Strong*
GPC + SM	Low	High	Complex*	Weak
EFL + SM	Medium	High	Simple	Medium*

GPC: Generalized Phase Contrast, HOT: Holographic Optical Tweezers, MO: Motorized objective or stage, SM: Scanning mirror, EFL: Electrically focus-tunable lens. * Depends on the number of traps.

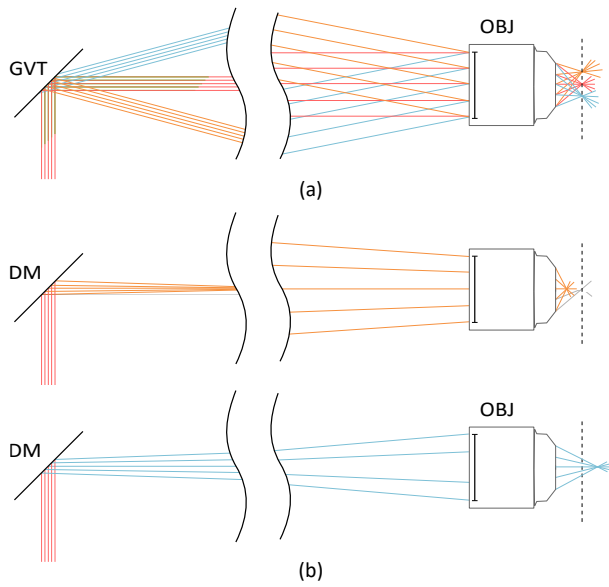


Fig. 1. (a) Schematic representation of how the laser beam will pivot around the objective's (OBJ) entrance aperture for small movements of the mirror galvanometer (GVT), creating the motion of the optical trap in the optical plane; (b) Schematic representation of the effect of focusing or defocusing the deformable mirror (DM) to change the z position of the traps. The size of the beam at the objective's entrance aperture remains the same, regardless of the degree of collimation of the incident beam.

A deformable mirror (DM) which can focus or defocus the beam is used on z . The deformable mirror and the galvanometer are positioned in a conjugate plane on the entrance aperture of the objective (OBJ). Hence, the laser beam will pivot around the entrance aperture of the microscope objective and retain the same degree of overfilling, independently of the angle or degree of collimation of the

incident beam, producing equally efficient and stable traps as much as possible [39]. Fig. 1 depicts this principle.

The deformable mirror (*PTT111 DM, Iris AO*) is a microelectromechanical component with 111 actuators and 37 piston-tip-tilt segments with an update rate of more than 2 kHz. Each segment has 700 μm diameter while the array has an aperture of 3.5 mm and with a maximum dynamic range (Stroke) of 5.8 μm . Electrostatic actuation allows precise positioning of each segment with nanometer and microradian resolution (wavefront resolution < 15 nm rms). The mechanical step-response speed is less than 200 μs (10-90%) and has high reflectance ($> 99.9\%$).

The segmented DM can effectively create smooth shapes, and it is used to control the degree of collimation of the laser beam. By synchronizing the orientation of the mirror galvanometer and the motion of the DM it is possible to displace the focal spot laterally and axially while maintaining the diffraction-limited performance. This axial scan implies a very low mechanical inertia, hence the z bandwidth is compatible with the galvanometer. The overall switching speed between 3D trap positions is in the same order of magnitude of equivalent 2D systems in the literature, as is shown below. Thus, it is possible to obtain very stable traps without introducing any significant aberrations.

The optical scheme of the system is shown in Fig.2.(a). The Gaussian laser beam (1070 nm) is guided into the inverted microscope through the galvanometer, the DM, and standard optical elements. Two afocal systems ($f_1:f_2$ and $f_3:f_4$) are used to conjugate the two actuators with the entrance aperture of the objective and to expand the laser beam. It's expanded in order to overfill (20%) the objective entrance to improve the trapping efficiency [26]. A picture of the whole platform is shown in Fig.2.(b).

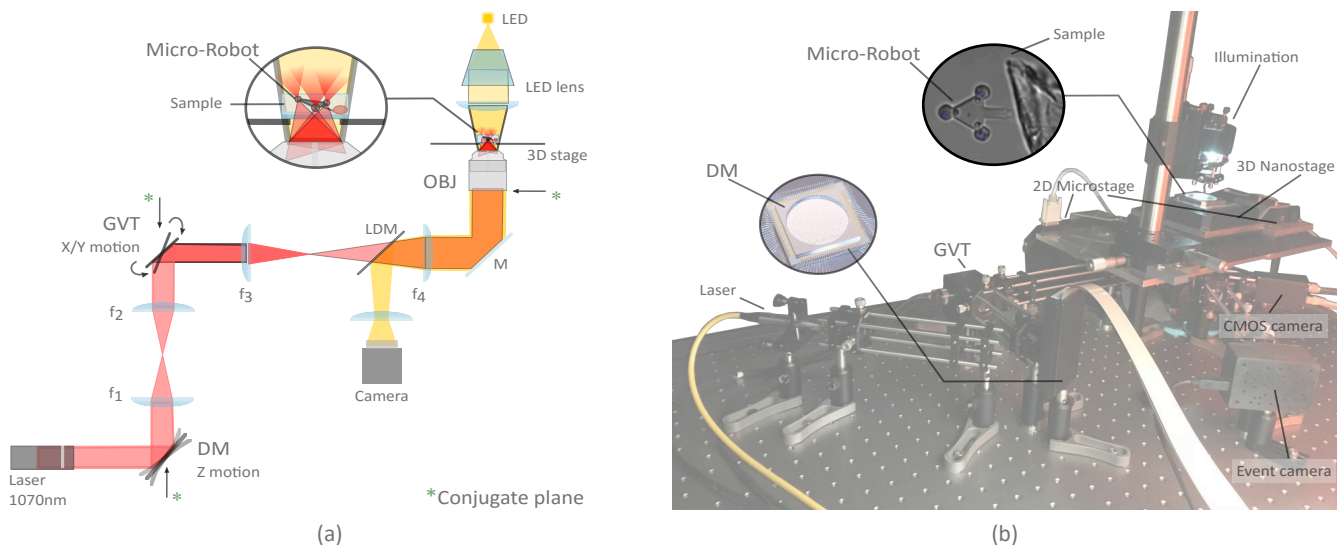


Fig. 2. (a) Optical path of the time-shared multi-trap actuation. The source is a 1070 nm laser with a maximum output of 10 W. The deformable mirror (DM) and the galvanometer (GVT) are positioned in a conjugate plane of the entrance aperture of the objective (OBJ) and used to control the axial and the planar positions respectively. The oil immersion objective (Olympus UPlanFLN 40x, NA 1.3) is used to produce the optical traps and to image the scene. The illumination (LED, 3 W) is reflected by a longpass dichroic mirror (LDM, 900 nm cutoff) into the CMOS camera (Basler, 659 \times 494 pixels). $f_1 = f_2 = 50$, $f_3 = 60$, $f_4 = 250$, M:Mirror. (b) Image of the optical trapping system with a close-up photograph of a Deformable Mirror (PTT111 DM, Iris AO) and a triangular optical robot. Two micro-stages (x - y) and a 3D nano-stage provide respectively coarse and fine positioning of samples.

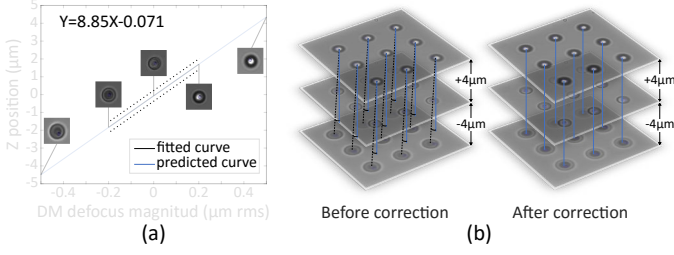


Fig. 3. (a) The axial position range of the system. The linear regression coefficients show the conversion between DM coordinates and the real displacement, as reported by the position sensor; (b) The correction in $x - y$ axes when a motion in z is generated.

The balanced distribution of power among different traps and the synchronization between the galvanometer and the DM constitutes a critical issue in the system. A hard real-time¹ control framework implemented in C++ is set up to manage the synchronization. A single PC (Intel Xeon core, 2.93 GHz) operating under a real-time Linux co-kernel and RTOS APIs Xenomai [40] gives satisfactory performances, without requiring any special hardware nor GPU. Synchronized parallel threads corresponding to the galvanometer and the DM run at hard real-time with fixed sampling rate. Given the very low response time of these components, near perfect synchronization is observed.

A. Calibration of the system

Precise positioning in 3D of each trap requires calibration between the optical path and real world coordinates. Using the microscope, $x - y$ calibration can be obtained quite straight forwardly, using any known distance. The precision in this case is limited by the optical properties of the microscope and the quality of the external gauge. The actuation sensitivities in $x - y$ axes are $37 \mu\text{m}/\text{deg}$ and $35 \mu\text{m}/\text{deg}$ respectively. The lateral workspace is limited by the range of view of the camera and is estimated as $56 \times 43 \mu\text{m}$.

The calibration in axial direction z is not an obvious task, as one can not rely upon the 2D optical feedback. An event based camera is used in this purpose, as previously described [41]. This sensor has a range of $\pm 2 \mu\text{m}$ around the focus plane with 5% SD. A $3 \mu\text{m}$ silica micro-sphere is trapped and displaced along the z axis, by varying the defocus magnitude of the DM from -0.5 to $0.5 \mu\text{m rms}$, while tracing the position of the bead as seen by the above mentioned sensor. 70,000 data points are recorded in the $4 \mu\text{m}$ range of the sensor, giving an excellent linear fit depicted in Fig.3. The working range of the axial displacement is estimated as $9 \mu\text{m}$ between the maximal and minimal defocusing position of the DM . This workspace depends on the current set-up and can be easily increased using a DM with larger stroke (eg. DMP40, Thorlabs).

Also, the initial calibration showed a cross-talk between planar and axial motions as shown in Fig. 3.b. This is due to a small misalignment in the light path, which is corrected in control, enabling independent motion of all three axes.

¹The "hard real-time" here indicates the high precision of task scheduling, which is controlled by real-time kernel in a patched Linux system.

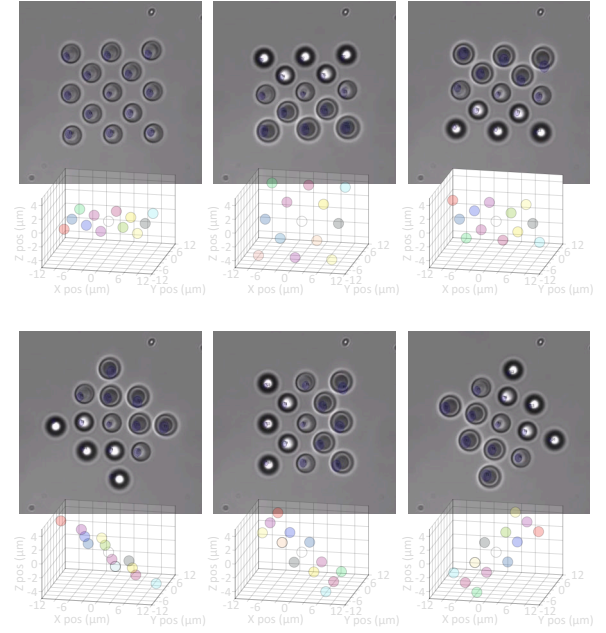


Fig. 4. Controlled movements of thirteen micro-beads arranged in a cube of $16 \times 16 \times 8 \mu\text{m}$

B. Evaluation of the system

The system allows a sampling rate of 2 kHz for the control of z axis for small displacements below $2 \mu\text{m}$. In order to exploit the full range of $9 \mu\text{m}$ allowed by the DM , the control loop is executed at 200 Hz. This bandwidth is in the same order of magnitude as the 2D mirror galvanometer (GVS002, Thorlabs), with full scale bandwidth of 250 Hz and 1 kHz for small angles ($\pm 0.2^\circ$). Note that the DM lacks position feedback and is controlled in open-loop, based on the calibration. The mirror galvanometer is controlled in closed-loop through electronics provided by the constructor with an angular resolution of 0.0008° .

The absence of external perturbations makes the synchronization between those 2 actuators reliable enough: the system allows the trapping and independent control of more than 15 micro-beads in different axial positions. Fig. 4 shows 13 micro-beads simultaneously trapped in 3D space, synchronously manipulated. The micro-spheres are arranged within a cube of $16 \times 16 \times 8 \mu\text{m}^3$. The laser power is 400 mW (measured at the laser output) and the shared irradiation time is set to 5 ms for each trap. These values of power and time-sharing were optimized experimentally. Table II summarizes the principal parameters of the system.

TABLE II
SUMMARY OF THE SYNCHRONIZED SYSTEM PARAMETERS

Actuation range	$50 \times 45 \times 9 \mu\text{m}^3$
Full scale bandwidth	200 Hz
Small scale ($\pm 2 \mu\text{m}$ in z) bandwidth	2 KHz
Latency	200 μs
Stable independent optical traps	> 15
Optical loss	< 3%

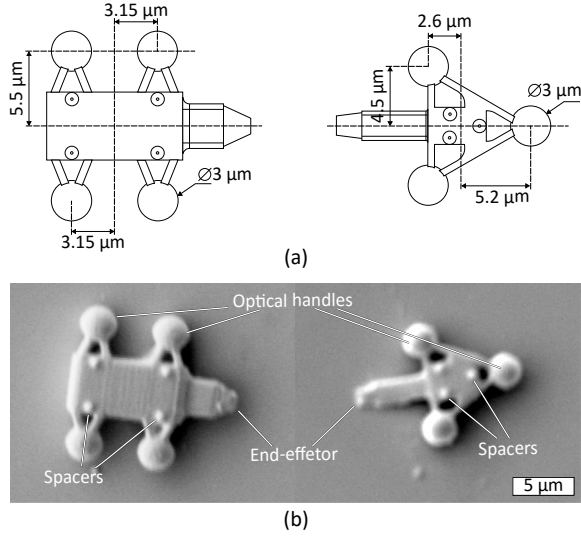


Fig. 5. (a) Schematic depictions with dimensions of two different optical robots; (b) Scanning electron microscopy (SEM) images of robots.

IV. 6-DOF TELEOPERATED OPTICAL ROBOTS

Optical robots are basically small inert structures, with spherical handles implemented at different locations. These can be custom designed for a particular experiment. This case is quite well adapted to a remote handling scenario: the operator will have full control of the robots and can flexibly carry out his task. The high bandwidth of the proposed system and the lack of any noticeable latency allow such a direct control to be easily implemented.

A. Fabrication of Robots

At least three 'handles' are necessary to induce complete spatial motion. Two types of optical robots have been designed, with three and four spheres of 3 μm diameter as optical handles (Fig. 5). Different spacers are attached on both sides of the robot to minimize the adhesion forces. They are fabricated through two-photon polymerization (2PP) (Nanoscribe Photonic Professional). Each robot can be printed with various end-effectors appropriate for different applications.

The robots are incubated in distilled water, 5% ethanol and 0.5% Tween20 solution to prevent the surface adhesion. For the experiments, micro-robots are transferred to a sample chamber

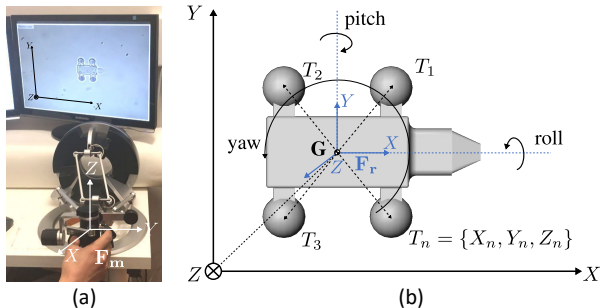


Fig. 6. (a) Master device and his reference frame. (b) Representation of robot's kinematics and frames used in the 3D control.

though an actuated microliter syringe, then sealed with another cover-slip, thus enclosed in a confined space.

B. Robot control

A (6+1) DoF master device (Omega.7, ForceDimension) is used to control the position of the robots (Fig. 6.a). The system allows to create traps on the fly, so the user can sequentially position traps on each handle and then control it in 6-DoF.

The robot kinematics were expressed in a local reference frame F_r attached to its body. The origin of this frame is a virtual point G in the center of rotation of the robot. Each optical handle is relative to the point G and defined with a 3D vector $T_n = \{X_n, Y_n, Z_n\}$ where n depicts the number of the trap (Fig. 6.b and Algorithm 1).

Algorithm 1 6-DoF teleoperated control of optical robots

Require : Initial traps position $T_n = \{X_n, Y_n, Z_n\}$ and center of rotation $G = \{X, Y, Z\}$; $i = 1$

0: **every 5 ms switch to next trap i+1**

1: **do for trap i**

2: Acquire position $P = \{px, py, pz\}$ and orientation $\Omega = \{rx, ry, rz\}$ of master device.

3: Calculate G : $G + P \times \text{gain_pos}$.

4: Update Rotation Matrix : $R[3][3] \leftarrow \text{Rot_Mat}(rx, ry, rz)$.

5: Calculate new trap position of trap i : $Np = R \times T_i$

6: Transform Np and G in mirror coordinates

7: Send Output : $M = Np + G$ to mirrors controllers

8: **end do**

1) *3D translations*: The reference frame is used to translate each trap, resulting in a uniform motion of the robot as depicted in Fig. 7. Motions of the master device are scaled down by 1×10^{-4} to control the 3D translation of the optical robot. In this configuration the workspace is limited to the field of view of the camera in $x-y$ and by the working space of the axial actuation.

An alternative control technique is implemented, where the operator moves the sample-chamber through the nano-stage. In this configuration, the robot has a fixed position in the camera view. Nano-stage can be driven in two modes, rate-control to explore all the sample chamber, and position-control to execute precise tasks.

2) *3D Rotations*: The orientation of the robot is controlled by the orientation of the master device with reference frame F_m . The rotation matrix R from F_m to F_r is calculated using the *Tait-Bryan angles* with $z-y-x$ convention (yaw, pitch

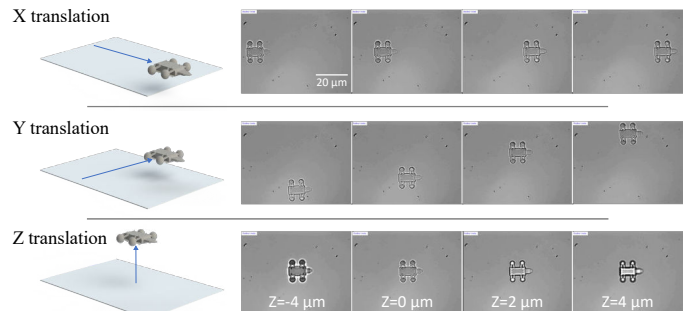


Fig. 7. Experimental validation of 3D translation control of Optical Robots.

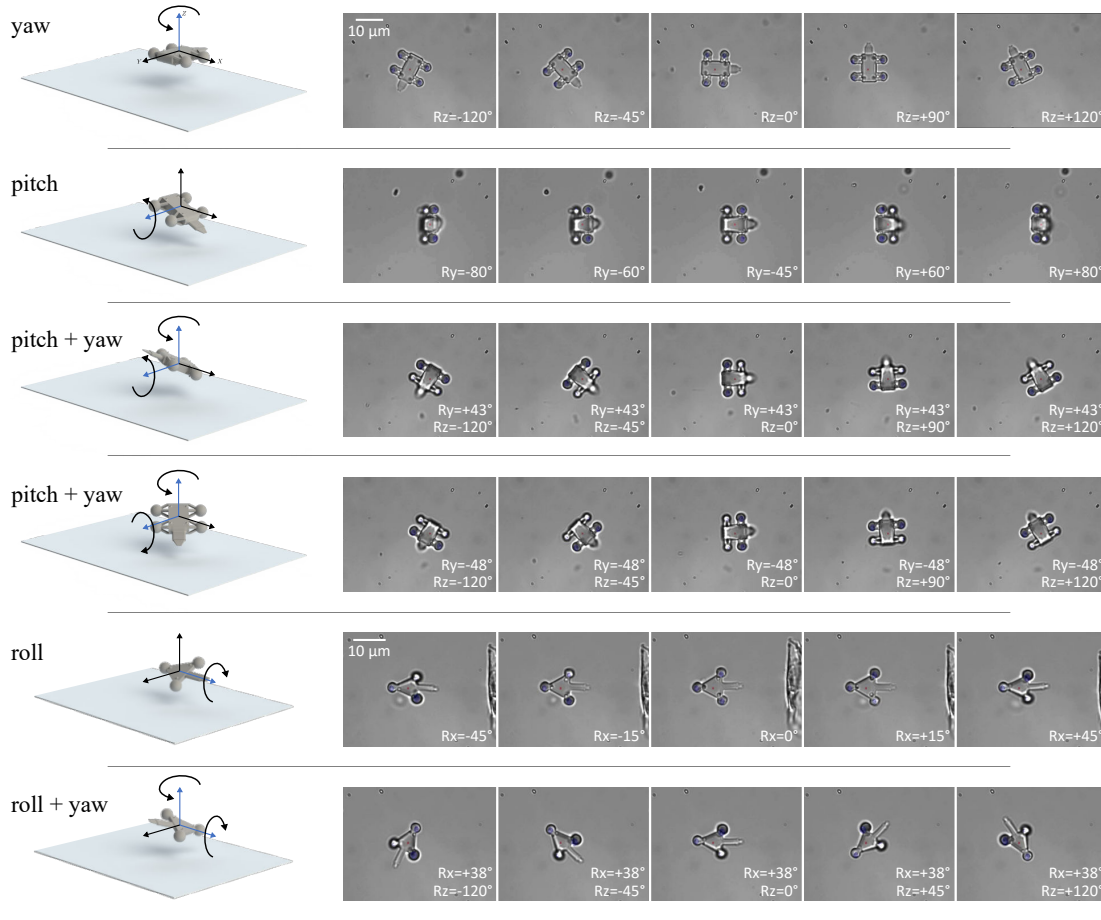


Fig. 8. Experimental validation of rotation control of Optical Robots.

and roll). Oriented 3D trap positions are calculated as $R \times T_n$. Fixed and mobile frames are coincident with zero angles. Figure 8 shows a succession of different rotations around all-three axes. The attached video² shows the 6-DoF control of the two different robots. Note that the footage is in real-time, not accelerated. True 6-DoF motion ability of an optical robot is successfully demonstrated.

The achievable orientation range depends naturally on the maximum distance separating optical handles and the center of rotation, and limited by the working space of the 3D actuation technique. The rotation around x (*roll*) is $\pm 35^\circ$ for four-handles robot and $\pm 45^\circ$ for three-handles robot. The rotation around y (*pitch*) is limited to $\pm 85^\circ$ in order to avoid the eventual occlusion between two traps in a vertical configuration. Around z (*yaw*) the rotation is virtually unlimited. It's artificially set to $\pm 120^\circ$ to match the handle rotation of the master device. Every DoF can naturally be controlled independently, coupled to another, or fixed. Note that every rotation can be controlled in speed rather than position, similarly to what was exposed above for translations.

²Please see the supporting information

V. DISCUSSION AND FUTURE WORK

A new design with a fast and efficient architecture to generate several independent optical traps in arbitrary 3D positions is presented here. Up to 15 stable traps are generated in a volume of approx. $50 \times 45 \times 9 \mu\text{m}^3$, with a high bandwidth (up to 200 Hz) and nanometric resolution. The proposed system takes advantage of a combination of a mirror galvanometer and a deformable mirror with high reflectance, and hence is aberration-free. The implementation of 3D trajectory control is straightforward and its low computational cost and latency makes it suitable to be exploited for closed-loop or interactive control schemes. This approach can be advantageously used in different applications where the orientation of microscopic objects (biological or synthetic) is needed, such as cell surgery applications, 3D tomographic imaging of living samples, optically driven micro-machines or micro-assembling in microfluidic devices.

Thanks to the capabilities of the method, and because of its stable and simple set-up design, 6-DoF control of an optical robot in a teleoperated scenario have been demonstrated. This is a significant illustration of new robotic applications that can benefit from the proposed 3D optical manipulation. Furthermore, the actuation method combined with an intuitive and flexible user interface could be used in complex biological

application where dexterous motions in 3D space is necessary. Since the optical-robot structures can be directly 3D printed according to the needs of a given experiment, each structure will have proper characteristics, and the system must have the capacity to adapt to this new tool. Proposing a fully automated control for each situation can be inefficient, as most of the protocols are not completely defined before the operation.

Possible applications of teleoperated 6-DoF optical robots include drug delivery tasks, pushing, 3D orientation of biological samples, 3D sensing, localized mechanical stimulation of single cells and any application requiring dexterous cell handling. More advanced functionalization (chemical, magnetic) of optical robots will take even further their capacity for micro-manipulation.

In addition to provide the axial motion, the *DM* can be also used for shaping the beam structure. Compared to a *SLM*, it has excellent wavelength response and speed but lower spatial resolution. Combined, the wave shaping capabilities of the *DM* and the lateral deflection of the galvanometer, it will be possible to create more sophisticated motions and functions of the trapped objects. This real-time multi-trap technique can also be used in applications requiring a rapid generation of light beams such as optogenetics, structured light for microscopy or optical communications [42].

In future work, we plan to study the indirect 3D orientation of cells through optical robots with different end-effectors. We anticipate that the 3D micro-manipulation of biological samples without direct exposition to the laser beam will contribute to many cellular applications, where the cell rotation task is a required step, such as nuclear transplantation, embryo micro-injections and polar-body biopsy [43]. We also plan to extend this 6-DoF control to several simultaneous optical robots for collaborative tasks. Also, the sensor used for the calibration can be exploited for indirect 3-axis force measurements, similarly to what was presented [41]. This will open the way to force control of the robots, as well as to haptic feedback teleoperation where pico-Newton scale forces can be rendered to the user.

ACKNOWLEDGMENT

The authors would like to thank Dr. Youen Vitry and the Micro-Bio-Mechatronics Research Unit of the Ecole Polytechnique de Bruxelles for discussions and the printing of micro-robots.

REFERENCES

- [1] J. Li, B. E.-F. de Ávila, W. Gao, L. Zhang, and J. Wang, "Micro/nanorobots for biomedicine: Delivery, surgery, sensing, and detoxification," *Sci. Robot.*, vol. 2, no. 4, 2017.
- [2] A. Ashkin, J. Dziedzic, and T. Yamane, "Optical trapping and manipulation of single cells using infrared laser beams," *Nature*, vol. 330, no. 6150, pp. 769–771, 1987.
- [3] S. P. Gross, "8 application of optical traps in vivo," *Methods in enzymology*, vol. 361, pp. 162–174, 2003.
- [4] H. Zhang and K.-K. Liu, "Optical tweezers for single cells," *Journal of The Royal Society Interface*, vol. 5, no. 24, pp. 671–690, 2008.
- [5] M.-C. Zhong, X.-B. Wei, J.-H. Zhou, Z.-Q. Wang, and Y.-M. Li, "Trapping red blood cells in living animals using optical tweezers," *Nature communications*, vol. 4, p. 1768, 2013.
- [6] R. Diekmann, D. L. Wolfson, C. Spahn, M. Heilemann, M. Schüttelz, and T. Huser, "Nanoscopy of bacterial cells immobilized by holographic optical tweezers," *Nature communications*, vol. 7, p. 13711, 2016.
- [7] Y.-c. Lin, H.-C. Chen, H.-Y. Tu, C.-Y. Liu, and C.-J. Cheng, "Optically driven full-angle sample rotation for tomographic imaging in digital holographic microscopy," *Optics letters*, vol. 42, no. 7, pp. 1321–1324, 2017.
- [8] S. Chowdhury, A. Thakur, P. Svec, C. Wang, W. Losert, and S. K. Gupta, "Automated manipulation of biological cells using gripper formations controlled by optical tweezers," *IEEE Transactions on Automation Science and Engineering*, vol. 11, no. 2, pp. 338–347, 2014.
- [9] S. Maruo and J. T. Fourkas, "Recent progress in multiphoton micro-fabrication," *Laser & Photonics Reviews*, vol. 2, no. 1-2, pp. 100–111, 2008.
- [10] S. Maruo and H. Inoue, "Optically driven micropump produced by three-dimensional two-photon microfabrication," *Applied Physics Letters*, vol. 89, no. 14, p. 144101, 2006.
- [11] H. Maruyama, T. Fukuda, and F. Arai, "Functional gel-microbead manipulated by optical tweezers for local environment measurement in microchip," *Microfluidics and Nanofluidics*, vol. 6, no. 3, p. 383, 2009.
- [12] S. Fukada, K. Onda, H. Maruyama, T. Masuda, and F. Arai, "3d fabrication and manipulation of hybrid nanorobots by laser," in *Robotics and Automation (ICRA), 2013 IEEE International Conference on*. IEEE, 2013, pp. 2594–2599.
- [13] D. Phillips, M. Padgett, S. Hanna, Y.-L. Ho, D. Carberry, M. Miles, and S. Simpson, "Shape-induced force fields in optical trapping," *Nature Photonics*, vol. 8, no. 5, p. 400, 2014.
- [14] M. J. Villangca, D. Palima, A. R. Bañas, and J. Glückstad, "Light-driven micro-tool equipped with a syringe function," *Light: Science & Applications*, vol. 5, no. 9, p. e16148, 2016.
- [15] J. Köhler, S. I. Ksouri, C. Esen, and A. Ostendorf, "Optical screw-wrench for microassembly," *Microsystems & Nanoengineering*, vol. 3, p. 16083, 2017.
- [16] A. Bolopion, B. Cagneau, D. S. Haliyo, and S. Régnier, "Analysis of stability and transparency for nanoscale force feedback in bilateral coupling," *Journal of Micro-Nano Mechatronics*, vol. 4, no. 4, p. 145, 2008.
- [17] C. Leung, Z. Lu, X. P. Zhang, and Y. Sun, "Three-dimensional rotation of mouse embryos," *IEEE Transactions on Biomedical Engineering*, vol. 59, no. 4, pp. 1049–1056, 2012.
- [18] J. E. Curtis, B. A. Koss, and D. G. Grier, "Dynamic holographic optical tweezers," *Optics communications*, vol. 207, no. 1-6, pp. 169–175, 2002.
- [19] R. L. Eriksen, P. C. Mogensen, and J. Glückstad, "Multiple-beam optical tweezers generated by the generalized phase-contrast method," *Optics letters*, vol. 27, no. 4, pp. 267–269, 2002.
- [20] S. Fukada, K. Onda, H. Maruyama, T. Masuda, and F. Arai, "3d fabrication and manipulation of hybrid nanorobots by laser," in *Robotics and Automation (ICRA), 2013 IEEE International Conference on*. IEEE, 2013, pp. 2594–2599.
- [21] B. Cao, L. Kelbauskas, S. Chan, R. M. Shetty, D. Smith, and D. R. Meldrum, "Rotation of single live mammalian cells using dynamic holographic optical tweezers," *Optics and Lasers in Engineering*, vol. 92, pp. 70–75, 2017.
- [22] J. Ng, Z. Lin, and C. Chan, "Theory of optical trapping by an optical vortex beam," *Physical review letters*, vol. 104, no. 10, p. 103601, 2010.
- [23] T. Asavei, V. L. Loke, M. Barbieri, T. A. Nieminen, N. R. Heckenberg, and H. Rubinsztein-Dunlop, "Optical angular momentum transfer to microrotors fabricated by two-photon photopolymerization," *New Journal of Physics*, vol. 11, no. 9, p. 093021, 2009.
- [24] J. Zhao, I. D. Chremmos, D. Song, D. N. Christodoulides, N. K. Efremidis, and Z. Chen, "Curved singular beams for three-dimensional particle manipulation," *Scientific reports*, vol. 5, p. 12086, 2015.
- [25] K. Kim and Y. Park, "Tomographic active optical trapping of arbitrarily shaped objects by exploiting 3d refractive index maps," *Nature communications*, vol. 8, p. 15340, 2017.
- [26] K. C. Neuman and S. M. Block, "Optical trapping," *Review of scientific instruments*, vol. 75, no. 9, pp. 2787–2809, 2004.
- [27] F. Arai, K. Yoshikawa, T. Sakami, and T. Fukuda, "Synchronized laser micromanipulation of multiple targets along each trajectory by single laser," *Applied Physics Letters*, vol. 85, no. 19, pp. 4301–4303, 2004.
- [28] D. Ruh, B. Tränkle, and A. Rohrbach, "Fast parallel interferometric 3d tracking of numerous optically trapped particles and their hydrodynamic interaction," *Optics express*, vol. 19, no. 22, pp. 21 627–21 642, 2011.
- [29] F. Arai, T. Endo, R. Yamuchi, and T. Fukuda, "3d 6dof manipulation of micro-object using laser trapped microtool," in *Robotics and Automation, 2006. ICRA 2006. Proceedings 2006 IEEE International Conference on*. IEEE, 2006, pp. 1390–1395.

- [30] F. Arai, T. Endo, H. Maruyama, T. Fukuda, T. Shimizu, and S. Kamiya, "3d manipulation of lipid nanotubes using laser trapped functional gel microbeads," in *Intelligent Robots and Systems, 2007. IROS 2007. IEEE/RSJ International Conference on*. IEEE, 2007, pp. 3125–3130.
- [31] Y. Tanaka, K. Hirano, H. Nagata, and M. Ishikawa, "Real-time three-dimensional orientation control of non-spherical micro-objects using laser trapping," *Electronics Letters*, vol. 43, no. 7, pp. 412–413, 2007.
- [32] Y. Huang, J. Wan, M.-C. Cheng, Z. Zhang, S. M. Jhiang, and C.-H. Menq, "Three-axis rapid steering of optically propelled micro/nanoparticles," *Review of Scientific Instruments*, vol. 80, no. 6, p. 063107, 2009.
- [33] G. Carmon and M. Feingold, "Rotation of single bacterial cells relative to the optical axis using optical tweezers," *Optics letters*, vol. 36, no. 1, pp. 40–42, 2011.
- [34] Y. Tanaka and S.-i. Wakida, "Controlled 3d rotation of biological cells using optical multiple-force clamps," *Biomedical optics express*, vol. 5, no. 7, pp. 2341–2348, 2014.
- [35] Y. Tanaka, "Double-arm optical tweezer system for precise and dexterous handling of micro-objects in 3d workspace," *Optics and Lasers in Engineering*, vol. 111, pp. 65–70, 2018.
- [36] F. Arai, K. Onda, R. Iitsuka, and H. Maruyama, "Multi-beam laser micromanipulation of microtool by integrated optical tweezers," in *Robotics and Automation, 2009. ICRA'09. IEEE International Conference on*. IEEE, 2009, pp. 1832–1837.
- [37] E. Avci, M. Grammatikopoulou, and G.-Z. Yang, "Laser-printing and 3d optical-control of untethered microrobots," *Advanced Optical Materials*, vol. 5, no. 19, p. 1700031, 2017.
- [38] R. Kampmann and S. Sinzinger, "Optical tweezers affected by monochromatic aberrations," *Applied Optics*, vol. 56, no. 5, pp. 1317–1326, 2017.
- [39] E. Fällman and O. Axner, "Design for fully steerable dual-trap optical tweezers," *Applied Optics*, vol. 36, no. 10, pp. 2107–2113, 1997.
- [40] A. Barbalace, A. Luchetta, G. Manduchi, M. Moro, A. Soppelsa, and C. Taliercio, "Performance comparison of vxworks, linux, rtai, and xenomai in a hard real-time application," *IEEE Transactions on Nuclear Science*, vol. 55, no. 1, pp. 435–439, 2008.
- [41] M. Yin, E. Gerena, C. Pacoret, S. Haliyo, and S. Régnier, "High-bandwidth 3d force feedback optical tweezers for interactive biomanipulation," in *Intelligent Robots and Systems (IROS), 2017 IEEE/RSJ International Conference on*. IEEE, 2017, pp. 1889–1894.
- [42] H. Rubinsztein-Dunlop, A. Forbes, M. V. Berry, M. R. Dennis, D. L. Andrews, M. Mansuripur, C. Denz, C. Alpmann, P. Banzer, T. Bauer *et al.*, "Roadmap on structured light," *Journal of Optics*, vol. 19, no. 1, p. 013001, 2016.
- [43] Q. Zhao, M. Sun, M. Cui, J. Yu, Y. Qin, and X. Zhao, "Robotic cell rotation based on the minimum rotation force," *IEEE Transactions on Automation Science and Engineering*, vol. 12, no. 4, pp. 1504–1515, 2015.